

Review

# Recent Progress of Molecularly Imprinted Optical Sensors

Xianzhi Huang, Ling Xia and Gongke Li \* 

School of Chemistry, Sun Yat-sen University, Guangzhou 510006, China

\* Correspondence: cesgkl@mail.sysu.edu.cn; Tel.: +86-20-39339782

**Abstract:** Molecularly imprinted polymers (MIPs) have been widely utilized in the field of sensing due to their specific and high affinity towards target molecules. Combining the selective preconcentration capability of MIPs and the rapid quantitation merit of optical analytical techniques, MIP optical sensors have been applied to the analysis of various kinds of samples and have received considerable attention in recent years. In this review, we overviewed the progress of MIP sensors in combination with various optical detection methods, including fluorescence, surface plasmon resonance, Raman scattering, and chemiluminescence. The construction, characterization, working principle, and application of four kinds of MIP optical sensors are covered in detail. Finally, the opportunities and challenges currently encountered by MIP optical sensors are summarized.

**Keywords:** molecularly imprinted polymer; optical sensor; SERS; plasmonic; fluorescent; chemiluminescence

## 1. Introduction

Molecularly imprinted polymers (MIPs) are polymers possessing binding sites that recognize imprinted molecules. Since Arshady and Mosbach reported their simple template strategy for the synthesis of substrate specific polymers, which is based on complementary interactions [1], many scientists have used this strategy to construct MIP materials. In analytical chemistry, MIPs have been applied in chromatography, electrophoresis, catalysis, and chemical sensing [2–4]. An increasing number of researchers have begun to use MIPs with good selectivity as recognition elements of sensors, and many of them proposed the idea of combining MIPs with optical sensors.

Optical sensors have attracted considerable attention due to their advantages, including simple visual identification, real-time detection, low cost, high sensitivity for analytes, and portable analytical equipment [5], which is complementary to the high selectivity of MIPs and meets the needs of contemporary analysis and detection. Optically active materials can be easily combined with MIPs in a covalent or non-covalent coupling manner. When the MIP adsorbs the target molecule, the structure of the system will undergo certain changes, which will also result in certain changes to the optically active material, and, finally, reflect the change of the optical signal. The excellent matching between MIP materials and optical sensors causes MIP optical sensors to stand out in the fields of food safety, biosensing, environmental monitoring, daily chemical quality control, and so on.

In recent years, an increasing number of researchers have steered their attention toward MIP optical sensors. In terms of the types of optical signals used by the sensors, MIP optical sensors can be mainly divided into fluorescence sensors, surface plasmon resonance (SPR) sensors, surface-enhanced Raman scattering (SERS) sensors, and chemiluminescence (CL) sensors. According to the number of entries in *Web of Science* search results' (from January 2012 to December 2022), an increasing number of MIP optical sensors have been reported, and the number of publications in recent years has remained high, as can be seen in Figure 1. Fluorescence sensors are the most studied and mature [6], followed by other types of sensors, and there are constant innovations in the field. In this review, we examined the development of MIP optical sensors over the past five years, and summarized the construction, fabrication process, working principle, and typical applications of various



**Citation:** Huang, X.; Xia, L.; Li, G. Recent Progress of Molecularly Imprinted Optical Sensors. *Chemosensors* **2023**, *11*, 168. <https://doi.org/10.3390/chemosensors11030168>

Academic Editors: Verónica Montes García and Alexander Castro Grijalba

Received: 20 January 2023  
Revised: 21 February 2023  
Accepted: 27 February 2023  
Published: 1 March 2023



**Copyright:** © 2023 by the authors. Licensee MDPI, Basel, Switzerland. This article is an open access article distributed under the terms and conditions of the Creative Commons Attribution (CC BY) license (<https://creativecommons.org/licenses/by/4.0/>).

MIP optical sensors (presented in Figure 2). Finally, the current challenges and future development trends of MIP optical sensors are analyzed, in order to pave the way for more applications of MIP optical sensors over a wider field.

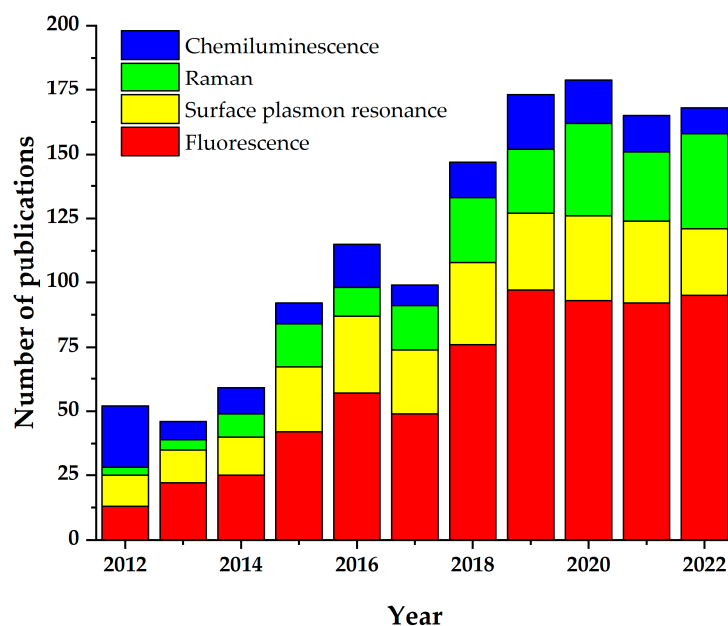


**Figure 1.** Number of publications with the keywords of molecularly imprinted fluorescence/surface plasmon resonance/Raman/chemiluminescence sensors. The data were collected from January 2012 to December 2022 according to the *Web of Science*.

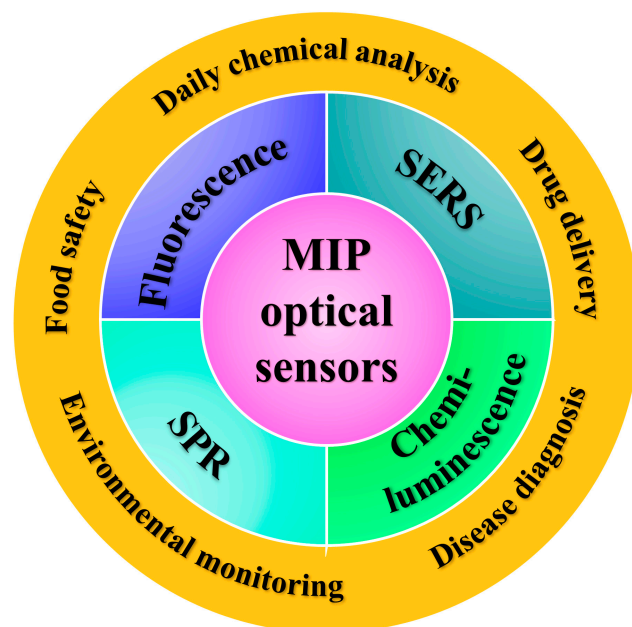


**Figure 2.** Schematic illustration of MIP optical sensors for application.

## 2. Molecularly Imprinted Optical Sensors

MIP optical sensors produce different optical responses under the condition of the presence or concentration of the substance to be detected. To this end, the construction of MIP optical sensors mainly incorporates the following aspects. For analytes that have intrinsic optical properties, especially those that can produce fluorescence [7], MIPs can be directly used as the “catcher” of target molecules, and then the intensity or change of relevant optical signals can be measured. For substances that have no optical properties

or have optical properties that are difficult to detect, the relationship between substance concentration and optical signal can be established by various means. The first is to pair the target molecule with the group or molecule having a strong optical response through covalent or non-covalent interactions. Then, the signal of the molecule or groups of molecules exhibiting strong luminescence can be detected [8]. The second is to introduce materials that can enhance the optical response of the target, and combine such materials with MIP properly, which is particularly common in the application of SERS detectors [9]. The third is to properly combine MIP with another material with an optical response. Through the combination of the target molecule and MIP, the performance of the optical response material is affected, so as to produce the change of signal. This is the classic principle of SPR sensors [10]. Due to different strategies, the preparation of sensors will be different. Generally, the optical active material and MIP in the sensor can be synthesized successively or co-synthesized. The elution of template molecules is then performed.

The functional monomers used to form the MIP should be able to interact strongly with the template molecules. Methacrylic acid contains a carboxyl group, which can react via ionic bonding with an amino group, as well as with an amide group via hydrogen bonding, so it is widely selected as the functional monomer of MIPs. Similarly, methyl methacrylate can be used for neutral template molecules. Vinylpyridine is a functional monomer that performs well for some acidic template molecules. The amide functional group of acrylamide can bond with peptides in proteins to produce a strong hydrogen bond, which is widely used in MIPs for proteins. In addition, functional monomers commonly used include MAPA, which can produce hydrophobic interactions; dopamine, which has good biocompatibility; and APTES, which is widely used in silicon MIPs.

After the preparation of the sensor, it is necessary to characterize it to ensure that its structure and properties conform to the design. The chemical composition and surface morphology of the sensor system are two key points of characterization. For example, UV-vis-NIR spectroscopy can be used to determine whether the distribution of optical active materials, such as nanoparticles, has changed and whether the template molecules have been removed [11]. SEM, TEM, and AFM are usually used to observe the surface morphology of materials [12]. Ellipsometry can characterize the thickness of the MIP layer [13]. Molecular components on the sensor can be viewed with a SERS spectrum to judge whether impurities and template molecules are removed [14].

Generally, MIP optical sensors are better than non-imprinted polymer (NIP) optical sensors in terms of sensitivity, detection limit, and selectivity, factors which are often used to explain the rationale for using MIPs. As reported by Göktürk and coworkers, the selectivity of a MIP-based SPR sensor toward guanosine was nearly three times that of a NIP-based sensor. The sensitivity and detection limits of the MIP-based sensor are also of great advantage [15]. To explain this phenomenon, computational simulations are often used. Common quantum chemistry calculation software, such as Gaussian, Chem3D, etc., are often used for simulation [8,16]. The sizes of the MIP cavities and the target molecule are obtained, and the matching between the synthesized MIP and the target molecule is often illustrated from the perspective of volume. To calculate the chemical binding energy between the groups in the MIP cavities and the target molecular groups, the degree of affinity between the target molecule and the MIP can be indicated. For optically active or enhanced materials, such as various metal nanoparticles, computational simulations, especially energy level calculations, are used to account for the forces between them and the MIP or target molecule, to determine their luminescence or enhancement capabilities. The intensity of the electric field between the nanoparticles can also be calculated to illustrate the enhancement effect of the optical signal [17].

The reusability and stability of the sensor are important properties. A sensor with good durability can greatly save the resources required for sensor preparation, so the sensor has economic practicability. According to literature reports, many MIP optical sensors have a certain durability. They can be reused many times after a certain regeneration process. Under the right conditions, they can be stored for quite a long time. Generally,

this can be attributed to the protective effect of MIPs. Optically active materials combined with MIPs are less susceptible to the external environment, which means that they neither break off easily when being cleaned nor react easily with destructive substances in the environment, which is helpful in maintaining the response strength and stability of MIP optical sensors [18]. However, the protection is somewhat limited. Under the influence of liquid shock and ultrasound during the regeneration procedure, the MIP will inevitably flake off and its cavities may be damaged [19]. This will lead to a decrease in the adsorption capacity of the MIP to the target molecule, which will also disengage or deactivate the optically active material to which it is bound. Among the reusable MIP optical sensors reported so far, the performance of most of them decreases significantly after more than ten uses. Of course, research is currently being undertaken to overcome this issue. For example, Jia et al. polymerized molecularly imprinted microspheres in situ on magnetic graphene, enabling the microspheres to bind firmly to magnetic graphene. The magnetic complex can be reused more than 30 times in a chemiluminescent sensing system, providing excellent durability [20]. Li et al. developed a molecularly imprinted SERS substrate with a self-cleaning function. The substrate can be exposed to ultraviolet light to remove template molecules without additional cleaning procedures which may cause the destruction of the sensing structure, so that it can maintain a high adsorption capacity after several cyclic tests [21].

### 2.1. Construction of MIP Optical Sensors

Because of different detection principles, the construction processes of MIP optical sensors based on fluorescence, SPR, SERS, or CL differ greatly. Here, we introduce the basic structure and preparation of four types of sensors mentioned above.

#### 2.1.1. Molecularly Imprinted Fluorescence Sensors

Molecularly imprinted fluorescence (MIF) sensors, which are prepared by combining MIPs with fluorescence sensors, show excellent sensitivity and are widely used in the detection of various substances [22]. When a certain concentration of the target object is combined with the MIP through specific recognition sites, the physical or chemical properties of the sensor system will be changed, and, thus, the fluorescence intensity will be changed. Therefore, by monitoring the change of the fluorescence spectrum, we can determine the concentration of the target in the system to be tested. The prepared MIF sensor not only exhibits a good selectivity and stability of MIPs, but also has the advantage of a high sensitivity of fluorescence detection. In practical applications, there is no need to use expensive instruments and complex sample pretreatments; thus, the rapid detection of complex samples with high sensitivity and the rapid development in sample detection can be enabled.

For fluorescent analytes, it is usually only necessary to capture them directly using MIPs. The fluorescent analyte, ciprofloxacin, was captured by an MIPs@PEGDA detector, as reported by Huang et al. [12]. The modification process for this sensor is given in Figure 3. For non-fluorescent analytes, there are two common ideas for the construction of MIF sensors. One is to use functional monomers with fluorescence for imprinting, forming MIPs with fluorescence. Another is to combine fluorophore materials, such as quantum dots (QDs) and carbon dots (CDs), with conventional MIPs.

The selection of fluorescent materials is critical. Fluorescent materials include organic dyes, QDs, CDs, and other novel fluorescent materials. Organic dyes have advantages of multiple varieties, rich colors, a convenient access, and a small size, but have the shortcomings of a narrow excitation peak, a wide tail emission peak, poor stability, and easy photobleaching, so the sensitivity is limited. They are gradually being replaced by other new fluorescent materials.

In recent years, QDs and CDs have been widely explored. QDs has the characteristics of a high emission quantum yield, excellent optical stability, and high photoluminescence efficiency. One of the advantages of QDs is that they can be customized at the nanoscale,

with adjustable properties, such as composition, size, and surface modification [23]. CDs have the characteristics of a low toxicity, environmental friendliness, and good water solubility, so they will be more widely used in the field of efficient identification and determination of target molecules in the future. For example, Zhang and colleagues proposed an MIF sensor combining l-cysteine-modified zinc sulfide QDs and magnetic nanoparticles. The sensor presented good linearity and a limit of detection (LOD) of 4.53 nmol/L for lysozyme [24].

Metal nanoclusters (NCs) generally accumulate several to hundreds of metal atoms. Compared with larger nanoparticles, they exhibit excellent optical properties, such as an adjustable fluorescence emission, a high stability, a large Stokes shift, and a high fluorescence quantum yield [25]. Bahari and colleagues designed a sensing platform with NiNCs and CdNCs that have outstanding optical properties. The NCs were mixed with secondary antibodies of the target analyte, CA 15-3, to form a bioconjugate. The bioconjugate was then used to prepare an MIF immunosensor. The limit of detection (LOD) was 50  $\mu$ U/mL.

Nanoparticles (NPs) can also be a good candidate for fluorophore materials. As reported by Lu and colleagues, the fluorescence signal of HRP can be amplified when tetra(4-carboxyphenyl) porphyrin NPs dissolve into porphyrin molecules [26]. The MIFS prepared according to this property could be applied in the detection of HRP with an LOD of 0.042  $\mu$ g/L.

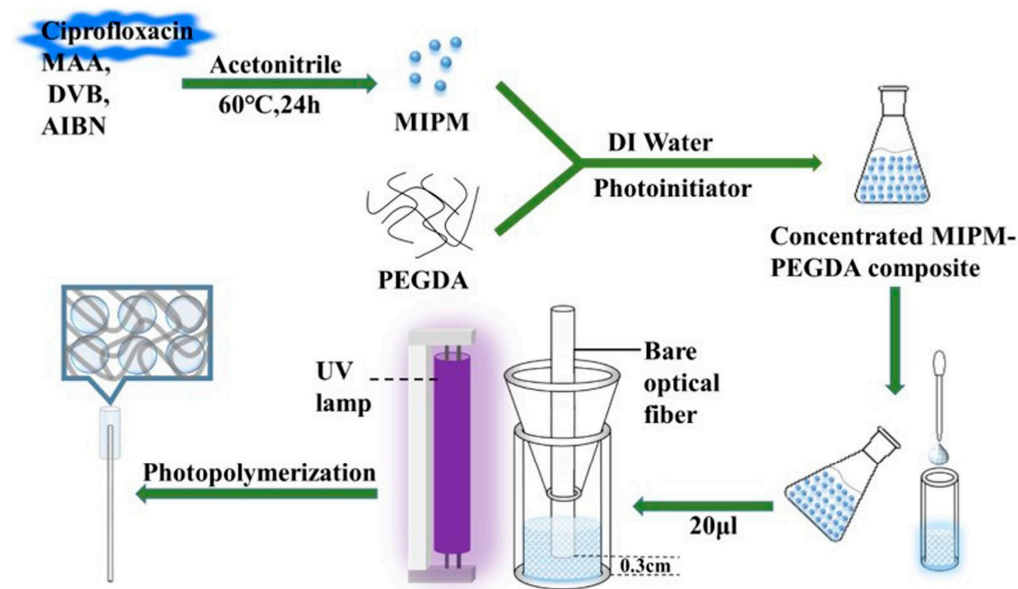


**Figure 3.** Modification of a MINs@PEGDA detector [12]. Copyright 2021 Elsevier (Amsterdam, The Netherlands).

In target analyte detection, the selective interaction between the fluorophore and the analyte can be expressed by the quenching or the enhancement of the fluorescence brightness signal, and the change of these signals is very sensitive to the dose, which can quantitatively detect differences in the analyte concentration at different selective interactions between fluorophores and analytes. Depending on the principle of selective interaction between fluorophores and analytes, MIF sensors are classed into three types: fluorescence resonance energy transfer (FRET), photoinduced electron transfer (PET), and inner filter effect (IFE) [27]. Fluorescence sensing itself has a high sensitivity and stability, and when combined with the selectivity of MIP, it is valuable. After many years of development, research on MIF sensors has remained a hot topic.

### 2.1.2. Molecularly Imprinted SPR Sensors

Surface plasmon resonance (SPR) is a physical optical phenomenon whose essence is free electron oscillation at the interface of media [28]. A small change in the surface of

the metal film can lead to a significant change in the SPR spectra [29]. This change can be due to the adsorption of the target molecule. Therefore, the SPR spectra can reflect the concentration changes of the analytes in contact with the surface of the metal film. In recent years, SPR sensors have attracted increasing attention, because their real-time, rapid detection, low cost, and other characteristics are needed in many practical situations [30].

The operation of an SPR sensor is dependent on various optical configurations [31]. The pioneering work by Kretschmann et al. led to the emergence of prism-based SPR detection systems [32]. Nowadays, prism SPR sensors are being brought to perfection. SPR sensing chips coated with thin layers of metal nanoparticles have been commercialized. Manufacturers have also been able to produce prism-based SPR sensors. One of the most common ways to combine a MIP with an SPR sensor is to coat or drop the MIP directly onto a precious metal-modified SPR sensor chip. A typical preparation process of a molecularly imprinted SPR (MISPR) chip is as follows [30]: (1) the functional monomer and the template molecule are formed into a precomplex; (2) the monomer, crosslinker, and AuNPs are added, followed by the addition of an initiator to initiate polymerization; (3) the monomer phase is dropped onto on a modified gold surface; (4) after photoinitiated polymerization, an imprinted membrane is formed on the chip; and, finally, (5) the chip is cleaned. The procedure mentioned above is shown in Figure 4a.

Prepolymerization time and spin coating speed are two main conditions that need to be controlled in the process of MIP synthesis [11]. The prepolymerization time affects the viscosity of the solution and further affects the thickness of the MIP coating. The spin coating speed directly affects the thickness. The thickness of the film needs to be such that the gold nanoparticles are completely coated, but not so that the contact between the gold nanoparticles and the target is unduly affected. In addition, the film thickness should be as uniform as possible to ensure the reproducibility of the detection results.

In recent years, optical fibers (OFs) have been increasingly used in sensors. According to the different materials, the main OFs in use are plastic OFs (POFs) and silicon dioxide OFs (SOFs). In a typical MIP OF-SPR sensor, a metal layer is sprayed between the MIP layers and the OFs. SPR occurs between the metal layer and the MIP layer at the dielectric interface, and the optical fiber plays the role of signal transmission [33]. Compared with the prism, the OF is more flexible and it usually costs less. The extensibility of the OF enables the optical sensor to be remotely controlled. These advantages of the OF satisfy the visions of intelligent sensing [31]. For example, in a study by Cennemo and colleagues [34], a POF was chosen to produce a D-shaped POF-SPR sensing platform, with covalently coupled nanoMIPs on the plasmonic surface (see Figure 4b). In the preparation process, a buffer layer containing photoresist was used to improve the adhesion ability of the gold film and the performance of the SPR sensor. The MIP POF-SPR platform can detect human transferrin with an LOD of 1.2 fmol/L with high selectivity.

In addition to prism and optical fibers, the use of other waveguides as optical transducers is an option. For example, as reported by Cennemo et al. [35], a spoon-shaped waveguide was applied in an SPR biochemical sensor. A gold nanofilm was layered on the waveguide to enable plasmon excitation. By combining an antibody and a nanoMIP, separated sensing areas on the spoon-shaped waveguide were functionalized, which provided a multi-sensor able to detect human serum albumin encompassing eight orders of magnitude of concentrations. Building nanogratings is also an alternative choice. A gold nanograting deposited on a PMMA chip was used in a MISPR sensor for BSA, as reported by Arcadio et al. [36].

The general process of sensing using the MIP plasmonic sensor is as follows [30]. A quartz halogen lamp laser is passed through a glass prism at right angles. A peristaltic pump is used to pass the liquid sample through the sensor surface. When the analyte sample reaches the surface of the SPR chip, the SPR sensor responds quickly, the refractive index change of the SPR sensor occurs on the thin metal layer, and the analyte–ligand interaction effectively destroys the plasma wave and generates a detectable signal. The signal value in the sensing map changes in direct proportion to the increase of the analyte

concentration, and it is possible to plot the change value of the refractive index  $\Delta R$  as a function of time.

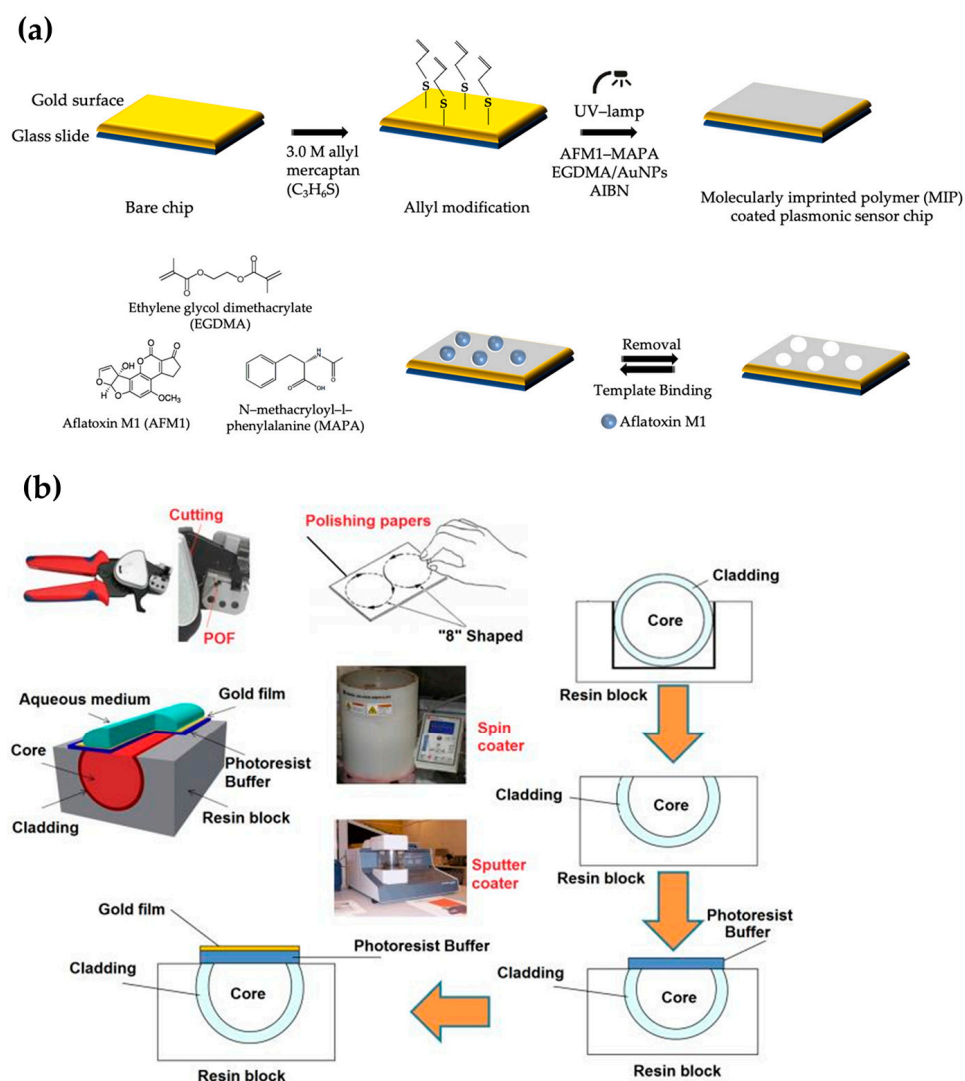


**Figure 4.** (a) Preparation of an MIP-SPR sensor chip [30] and (b) preparation of a POF-SPR sensor platform [34]. Copyright 2022 Elsevier (Amsterdam, The Netherlands).

### 2.1.3. Molecularly Imprinted SERS Sensors

Raman scattering is an optical phenomenon closely related to molecular properties. It originates from the inelastic collision between photons and molecules [37]. Since it was first observed by Raman and Krishnan in 1928 [38], and a way to enhance it was discovered in 1974 [39], Raman spectroscopy and the SERS technique have become an indispensable part of the field of spectral analysis.

In SERS detection, SERS substrates are undoubtedly the most important link. Whether the SERS substrates can effectively interact with the target objects and enhance the specific Raman signal largely determines the availability of the SERS substrates. However, traditional SERS substrates are almost entirely composed of precious metals; thus, they lack affinity for organic molecules and are susceptible to base interference [40]. This greatly limits the application of SERS in actual sample detection. To solve the problem, a wise choice is to combine SERS with MIPs. The addition of MIPs can greatly enhance the selectivity of the SERS base, and also isolate some interferences, thus improving the performance.

Morphologically, there are mainly two kinds of MISERS sensors [41]. One is particle-based sensors and the other is chip-based sensors. According to the relative position of

SERS substrates and MIPs, MIP can be covered on SERS-active materials, coated by SERS-active materials, or mixed with SERS-active materials; thus, MISERS sensors can be further divided into three categories. Regardless of the type of MISERS sensor, the relative content of MIPs and SERS-active materials should be properly regulated. When there is too much MIP or the thickness of the MIP layer is too high, it would make it difficult for the target molecules to approach the SERS substrate, thus resulting in the inability to generate a signal with sufficient strength. On the contrary, if the proportion of SERS-active materials is too high, less target molecules would be adsorbed by the sensor, which would also make the signal weak.

In order to properly combine the SERS-active material and the MIP, various methods have been reported. At present, an *ex situ* preparation method has been widely reported in the literature [37]. In this method, the SERS-active material is first synthesized and then the MIP is introduced. A typical scheme for the *ex situ* preparation is the construction of core-shell nanoparticles. As is shown in Figure 5, in a study by Ahmad and colleagues,  $\text{TiO}_2@Ag@MIP$  was fabricated for the detection of tryptamine. Firstly,  $\text{TiO}_2$  was dispersed in ultra-pure water, then  $\text{AgNO}_3$  was added and the mixture was reduced to obtain  $\text{TiO}_2@AgNPs$ . Subsequently, the target molecule (tryptamine) and the functional monomer (MAA) were added for prepolymerization. Finally, the crosslinker (EGDMA) and the initiator (AIBN) were added to complete the polymerization, and the  $\text{TiO}_2@Ag@MIP$  was obtained after washing off the template and other impurities. Core-shell imprinted nanoparticles had the advantages of a high surface-to-volume ratio and rapid binding kinetics, which was consistent with the requirement of SERS detection.

Another strategy for *ex situ* preparation is to combine the MIP with the target molecule and then try to transfer the target molecule to the SERS-active material to obtain the SERS signal. In this strategy, the MIP combined with the target molecules can be directly added or coated onto SERS-active materials. Kantarovich's team came up with a way to print MIPs droplets onto a SERS substrate using pipettes or nanopens, which can be used to directly monitor the absorption and release of the drug propranolol [42]. Target molecules on MIP can also be eluted onto SERS substrates. For example, Feng and colleagues used MIP to capture the analyte to process a solid-phase extraction. Then, it was deposited on the SERS substrate to be detected. This method is called the "capture-detection method" [43]; however, it is more complicated to some extent.

*In situ* preparation is a method to reduce metal ions directly into metal nanoparticles in MIPs. Currently, there are few studies on MISERS sensors constructed according to this method. This is because the *in situ* method usually requires larger quantities of noble metals and more stringent preparation conditions compared to the *ex situ* method. Moreover, MISERS sensors prepared using the *in situ* method do not have a significant advantage in terms of sensitivity. An advantage of *in situ* preparation is the ease of fabrication. In a study by Wang and coworkers,  $\text{AgNO}_3$  was directly added a mixture of a template, functional monomer, crosslinker, and initiator to process a one-pot synthesis of the sensor [44].

#### 2.1.4. Molecularly Imprinted CL Sensors

Chemiluminescence (CL), as the name suggests, is luminescence caused by chemical reactions. CL has been widely applied in immunoassays and clinical diagnosis for its extremely high sensitivity without the need of external light [45]. The application of pure CL is limited because of its poor selectivity and accuracy [46], but fortunately, there have been many technologies to help improve its performance.

To date, CL-ELISA methods, which use antibodies as recognition reagents, are frequently used to determine various analytes. However, they usually take a long time to synthesize antibodies, and most of the antibodies are not reusable, which greatly limits the application of conventional ELISA methods. Compared to antibodies, MIPs can also be used as a recognition reagent, and it has the advantages of a low cost, a short production time, and reproducibility [47]. Many scientists are exploring the possibility for MIPs to replace antibodies, and many MICL sensors have been developed.

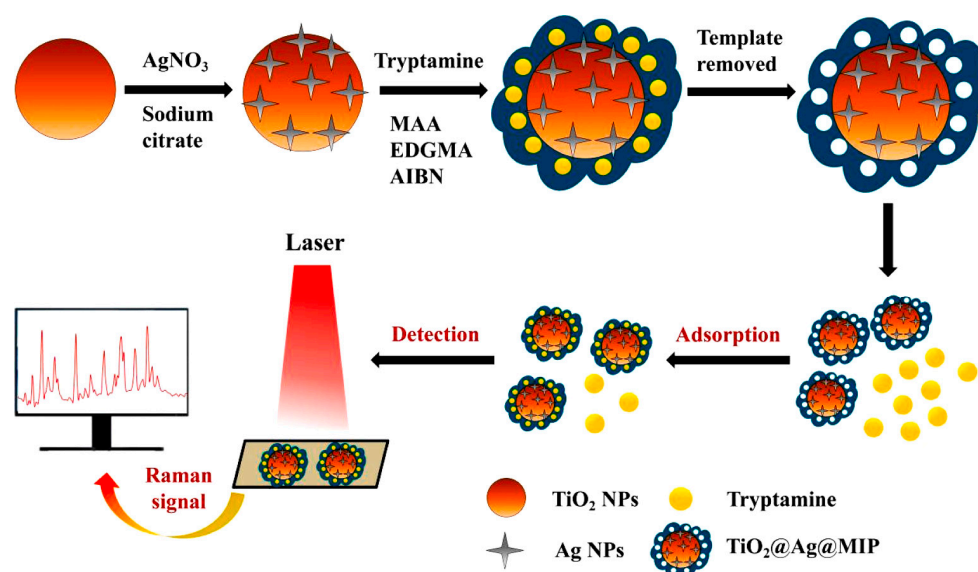


**Figure 5.** Fabrication of the TiO<sub>2</sub>@Ag@MIP SERS sensor and the detection of tryptamine [8]. Copyright 2022 Elsevier (Amsterdam, The Netherlands).

MICL sensors can be roughly divided into two categories according to the different ways of photochemical reaction. In some of the sensors, the photochemical reaction occurs directly in the medium. This type of sensor often uses microplate and microtitration techniques; hence, they are called MIP-based microplate/microtitration CL (MIMCL) sensors. Generally, the preparation of a MIMCL sensor includes three steps. Firstly, MIP particles and the “glue,” such as polyethylene glycol, are pipetted into the wells of a microplate. Secondly, the analyte solution is added to be absorbed. Thirdly, the wells are washed and the CL reagents are added to initiate light emission. The MIMCL sensor works in a very similar way to traditional ELISA, except that the specific recognition element is changed from antibodies to MIPs.

Other sensors use the principle of galvanic cells to allow photochemical reactions to occur on the electrodes, known as electrochemiluminescence (ECL). These types of sensors are called MIECL sensors. The most flexible aspect of the MIECL sensor is the electrode. In general, cyclic voltammetry can be used to deposit luminescent materials and synthesize the MIP on the electrode in sequence. By optimizing the amount of MIP and optically active materials, such as CDs, QDs, and NCs, on the electrode, the luminous efficiency and response sensitivity can be improved effectively [48].

A classic instance of MIMCL sensors is shown in Figure 6a [16]. For the preparation of an MIMCL sensor, the synthesis of the MIP and the preparation of labeled conjugates are the key steps. An enzyme-labeled conjugate was needed for competitive luminescence assays, so the UV–vis spectrum is often obtained to determine the success of the labeling. After washing, CL reagents are added into the wells of the microplates, then CL intensities are measured.

In Zhang and colleagues’ study [48], a common MIECL sensor construction method is shown (Figure 6b). After modifying CsPbBr<sub>3</sub>-QDs on the glassy carbon electrode (GCE), the MIP was electrodeposited. Before measurement, the sample solution was incubated for a short period of time, and the MIECL effect was recorded. For the MIECL system, the morphology and structure characterization of QDs or NCs is often undertaken, requiring TEM/SEM, FTIR, and UV–vis spectroscopy.

Computational simulation is often performed to prove the detection mechanisms of MICL sensors. For example, in He and colleagues’ study [47], computational simulation was performed to confirm the 3D conformation of seven dyes, and the binding energy of the MIP and analytes were calculated. From the data obtained by simulation, the team

obtained the conclusion that MIP recognition was mainly affected by the 3D conformation and the molecular size of the template.

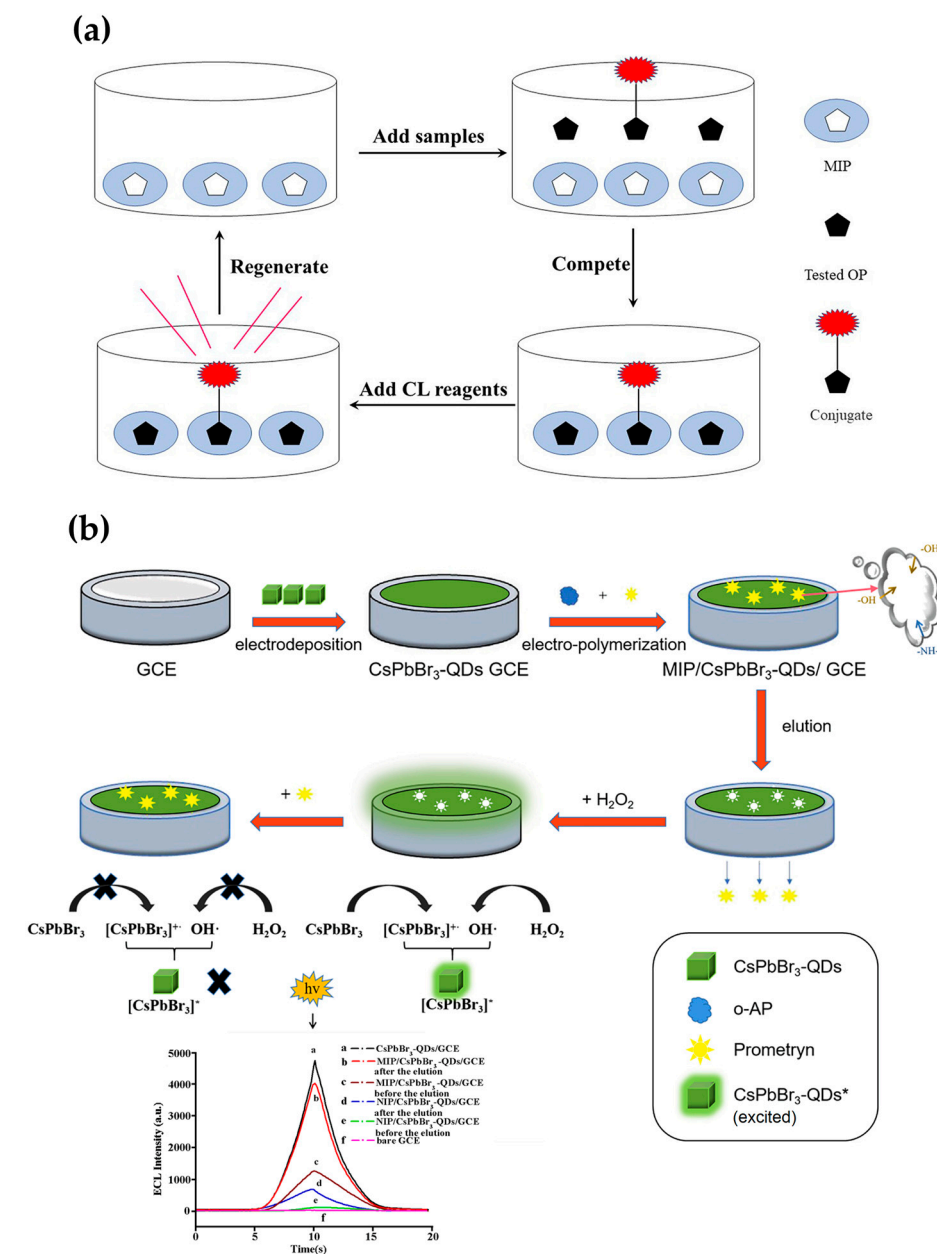


**Figure 6.** (a) Principle of MIP-based microtitration CL sensors in organophosphorus detection [16]. (b) Preparation of ultrasensitive ECL sensor for prometryn determination [48]. Copyright 2022 Elsevier (Amsterdam, The Netherlands).

## 2.2. Applications of MIP Optical Sensors

MIP optical sensors have shown excellent application prospects in many fields. Below, we briefly introduce the recent applications of MIP optical sensors mainly in food analysis, healthcare, and environmental safety.

### 2.2.1. Food Analysis

As an old saying goes, food is the paramount necessity of the people. Not only is food analysis an important topic in analytical chemistry, it is also a promising field for MIP optical sensors. Popular targets in food, such as toxins, dyes, and pesticide residues, are

mostly small molecules, which are suitable for selective detection by molecular imprinting technology, and it is easy to design an optical response system for them.

In the field of toxin detection, Zou and coworkers successfully applied MIP hydrogels (MIPGs) in the detection of zearalenone (ZON). As the functional monomer of the MIPGs, 4-VPY not only possesses fluorescence ability, but also absorbs ZON molecules via  $\pi$ - $\pi$  interactions with a high affinity. The sensor can be used in the detection of ZON in corn juice, with an LOD of 1.6  $\mu\text{mol/L}$  [49]. Although the LOD of the MIPGs sensor did not surpass that of antibody-based sensors or aptamer-based sensors, which are at the nmol/L or even pmol/L level, the sensor is much cheaper and has a longer service life; thus, it is more suitable for commercial use. Denizli's group developed nanofilm-based MISPR sensors for the detection of a series of toxins in foods. For example, an AFB1-imprinted nanosensor has been applied in the detection of AFB1 in peanut and corn samples, with an LOD of 1.04 pg/mL and a linear range across five orders of magnitude [50]. A much more sensitive response for AFB1 was obtained compared with other mycotoxins, and the relative selective coefficients for other tested mycotoxins ranged from 2.89 to 15.14. The team also realized MISPR sensors capable for the selective and sensitive detection of bacteria and viruses, such as T4 bacteriophages and Salmonella paratyphi, in drink samples [51,52]. Dye detection is undoubtedly an area where SERS methods excel. Wang and coworkers created a sandwich-like SERS substrate made of a Au array (AuA) and a MIP, as shown in Figure 7 [53]. When the target object R6G was adsorbed on the MIP recognition site near the gold array, a strong SERS signal could be generated. This sensing strategy enables MIPs to no longer restrict the mass transfer process and to improve the substrate reusability. Furthermore, structural analogues, such as RB, R123, and CV, are unable to interfere. The sensor exhibits an LOD of  $10^{-10}$  mol/L in water and juice samples, and it can be reused for at least six cycles. Towards drug residues in animals, Cai and colleagues firstly report an MICL sensor for eight benzimidazoles. Among them, mebendazole was finally chosen as the template to synthesize the MIP, and the sensor possessed an ultra-low LOD for mebendazole of 1.5 pg/mL. The sensor showed better recognition performance for benzimidazoles compared to all previously reported sensors, including some MIP-based or CL sensors, with regard to sensitivity and the recognition spectrum. Furthermore, the response of six potential competitors is negligible. The sensor has been applied in beef and mutton samples [54].

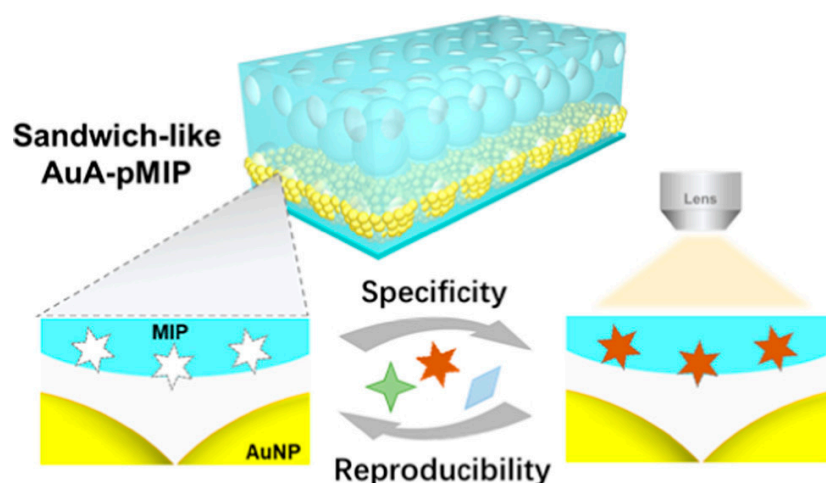


**Figure 7.** Working principle of the sandwich-like AuA-pMIP sensor. Reprinted with permission from reference [53]. Copyright 2020 American Chemical Society (Washington, DC, USA).

### 2.2.2. Healthcare

In the field of healthcare, the samples are mainly various human tissues or secretions, and the targets include various biomarkers and their derivatives. Testing of pharmaceutical ingredients is also an important aspect. Since the chemiluminescence method is often used

in biological analysis, the MIECL sensor has been reported more in this aspect. Some of the other types of sensors also show excellent analytical capabilities.

Hallaj's team used EuS NCs with excellent luminous properties as an optical signal source to form HIV DNA-imprinted membranes on the surface of ITO electrodes by electropolymerization. The MIECL sensor can achieve an ultra-sensitive detection of HIV-1 gene in human serum samples with a detection limit of  $0.3 \times 10^{-15}$  mmol/mL [55]. This is the first time that the MIECL method has been used to detect the HIV-1 gene, and its performance compares favorably with previous work related to the determination of the HIV-1 gene. Both the two-base mismatched DNA and noncomplementary DNA cannot generate an obvious signal, ensuring the specificity of the sensor. Hallaja's team have also developed a MIECL sensor to determine the quantity of creatine in serum and urine samples [56]. The photoluminescence properties of water-soluble NiNCs were firstly studied, and the NiNCs/TPrA system not only possessed excellent analytical performance (LOD =  $5 \times 10^{-4}$   $\mu$ mol/L), but also desirable reproducibility and stability. This can partly be attributed to the positive effects of the MIP. In a classic case of optical sensing, Lu's team developed an MIECL system based on biomass carbon, which was combined with a smartphone [57]. The smartphone can be used as both signal acquisition and signal processing units, which undoubtedly greatly improves the portability of the sensor. The strategy is shown in Figure 8. Li and coworkers developed a one-pot synthesized CDs-YVO<sub>4</sub>:Eu<sup>3+</sup> MIF ratiometric sensor [58]. The one-pot synthesis method greatly reduced the time and cost and improved the controllability. The MIP provided the attachment site of the target molecule 4-NP, while YVO<sub>4</sub>:Eu<sup>3+</sup> provided the fluorescent internal standard. The LOD was as low as 0.15  $\mu$ mol/L in human urine, and the determination had a high anti-interference ability. Saylan et al. showed a strategy to detect hemoglobin by using a nanofilm-based MISPR sensor [59]. An LOD of 0.00035 mg/mL was reported, and the sensor could be stored for as long as 27 months at room temperature, with only a 0.09% performance loss. Such durability is better than that of most antibody-based sensors. Arabi and colleagues developed an artful MISERS sensor in which the glass capillary was successively covered with a layer of Au nanostars (AuNSs) and a layer of MIP [60]. The MIP combined with target molecules can block access to Raman reporter molecules, so that the SERS spectrum changes. The idea of using the MIP layer to isolate reporter molecules is novel and provides a new role for MIPs in optical sensors.

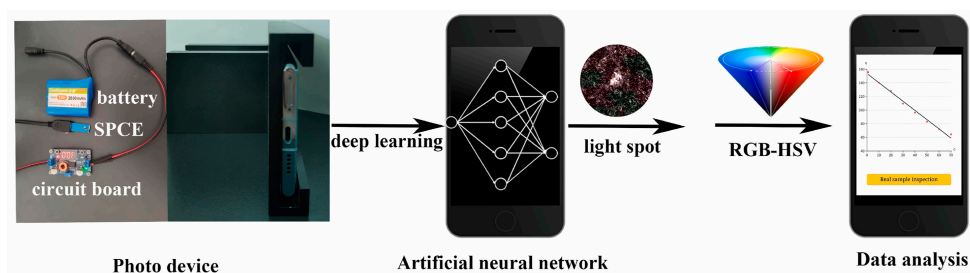


**Figure 8.** Illustration of a smartphone-based sensing platform [57]. Copyright 2022 Elsevier (Amsterdam, The Netherlands).

### 2.2.3. Environmental Safety

Environmental safety is closely related to people's lives. The task of environmental analysis is to detect related toxic and harmful substances in the environment, such as water, air, soil, and solid waste. Generally speaking, as long as the object can be converted into a liquid, it can be detected by MIP optical sensors.

For solid waste, Feng and colleagues first proposed an MIF sensor for the detection of TBBPA in electronic waste [61]. The CdTe QDs and the MIP layer are combined by silicon dioxide, which ensures that the QDs will not contact the interface to a maximum extent. The quenching effect of TBBPA is much higher than its analogues, showing good selectivity. Reaching an LOD of 0.3 ng/g, the precision and the recovery of the sensor are also competitive. Xue and coworkers proposed a MISERS sensor based on PDA-modified

MOFs@Ag for the detection of orange II [62]. In the process of sensor construction, MOFs and polydopamine played a role in adsorbing silver ions, while the MIP was used to adsorb orange II. Orange II can pass through the imprinting layer through the “gate effect” and bind to specific recognition sites inside. Even in a mixed system, orange II can preferentially bind to gold nanoparticles, leading to a high selectivity. The sensor has been used in the analysis of river water, and the LOD is lower than  $10^{-10}$  mol/L. Luo’s team developed a dual recognition strategy for metal ion detection by MIP [63]. They combined  $\text{Co}^{2+}$  with BSA to form complexes, which were then applied to molecular imprinting. The MWCNT/Cu/CDs system shown in Figure 9 will produce a strong optical signal when the BSA- $\text{Co}^{2+}$  is elution, and quench otherwise. This strategy overcomes the shortcomings of traditional MIP sensors, for which detecting metal ions is difficult. The sensor is suitable for the analysis of water, soil, and agricultural products samples, with an LOD of  $3.07 \times 10^{-10}$  mol/L.

The main information of MIP optical sensors developed in recent years can be seen in Table 1.

**Table 1.** Recent applications of MIP optical sensors.

Application	Sensor Type	Sensing System	Sample	Analytes	LOD	Ref.
	Fluorescent	MIP hydrogel	corn juice	ZON	1.6 $\mu\text{mol/L}$	[49]
		CDs@MIPs	milk	tetracycline	5.48 nmol/L	[64]
		fluorescent	ketchup	naringin	100 pmol/L	[65]
		MIP- $\text{Fe}_3\text{O}_4$ @ $\text{SiO}_2$	vodka	tau-fluvalinate	13.251 nmol/L	[66]
		MIPs-dye@ $\text{SiO}_2$	corn seed	alachlor	0.5 $\mu\text{mol/L}$	[67]
		F-MIP	water	bisphenol A	29 nmol/L	[68]
		M-R-MIPs@D-NPs				
	SPR	MIP coated Au chip	dried fig	ochratoxin A	0.028 ng/mL	[10]
		AgNPs based MIP chip	milk	penicillin G	1.2 fmol/L	[13]
		MIP coated Au chip	milk	aflatoxin M1	0.4 pg/mL	[30]
MIP coated Au chip		corn and peanuts	aflatoxin B1	1.04 pg/mL	[50]	
MINPs-Au		water	T4 bacteriophages	$1.4 \times 10^6$ CFU/mL	[51]	
	AuNPs-MIP chip	apple juice	salmonella paratyphi	0.49 ng/mL	[52]	
	MIP-Au-POF	drinking water	2-FAL, MW = 96.4	0.03 mg/L	[69]	
Food analysis	SERS	$\text{TiO}_2$ @Ag@MIP	spiked white vinegar	tryptamine	$4.85 \times 10^{-7}$ mol/L	[8]
		$\text{ZnO}$ @ $\text{TiO}_2$ @Ag@MIP	vinegar and prawn	histamine	$3.088 \times 10^{-9}$ mol/L	[9]
		AuNP/PDA-MIP	water, wine	phthalate plasticizer	$1.0 \times 10^{-10}$ mol/L	[18]
		Au Array-MIP	orange juice	R6G	$10^{-10}$ mol/L	[53]
		AuNPs-MIPs	sports drink	new red	$1.64 \times 10^{-7}$ mol/L	[70]
		MIP@BS (biogenic silica)	milk	$\beta$ -estradiol	0.073 ng/mL	[71]
		MIP- $\text{SiO}_2$ @Ag	water	bisphenol A	$1.46 \times 10^{-11}$ mol/L	[72]
		MIPs-AgNPs	milk	2,4-D	0.008 mg/kg	[73]
		Mag@MIP/Au	milk and tap water	2,4-D	0.00147 ng/mL	[74]
			CL	4IP-luminol- $\text{H}_2\text{O}_2$	milk	organophosphorus
4IP-luminol- $\text{H}_2\text{O}_2$	meat			chloramphenicol	2.0 pg/g	[20]
TCPO-IMZ- $\text{H}_2\text{O}_2$	egg			Sudan dyes	1.5 pg/mL	[47]
4IP-luminol- $\text{H}_2\text{O}_2$	meat			benzimidazoles	1.5 pg/mL	[54]
TCPO-IMZ- $\text{H}_2\text{O}_2$	milk			tetracyclines	1 pg/mL	[75]
MWCNT/MIP-QD	fish and seawater			cyfluthrin	0.05 $\mu\text{g/L}$	[76]
4IP-luminol- $\text{H}_2\text{O}_2$	meat			sulfonamides	1.0 pg/mL	[77]
TCPO-IMZ- $\text{H}_2\text{O}_2$	blank chicken			pyrethroids	0.010 $\mu\text{g/kg}$	[78]
4IP-luminol- $\text{H}_2\text{O}_2$	chicken, pork and fish			chloramphenicol	-	[79]
luminol- $\text{H}_2\text{O}_2$	spinach			monocrotophos	0.001 mg/L	[80]
4IP-luminol- $\text{H}_2\text{O}_2$	chicken and pork	amantadine and rimantadine	1.0 pg/mL	[81]		
CdTe QDs, $\text{H}_2\text{O}_2$	vegetable	clopyralid	$4.1 \times 10^{-12}$ mol/L	[82]		

Table 1. Cont.

Application	Sensor Type	Sensing System	Sample	Analytes	LOD	Ref.
Healthcare	Fluorescent	MNP/QD@MIPs	urine and egg white	lysozyme	$4.53 \times 10^{-3}$ mol/L	[24]
		FL-MMIPs	cell	CA 125 and CA 15-3	50 $\mu$ U/mL	[25]
		C-Y@MIPs	water and urine	4-nitrophenol	0.15 $\mu$ mol/L	[58]
		CD@SiO <sub>2</sub> @MIP	urine	bovine hemoglobin	0.155 $\mu$ mol/L	[83]
		QDs embedded MIM	human serum and saliva	lysozyme	10.2 nmol/L	[84]
		FL-MIF	Euphorbia fischeriana Steud	Ebracteolata compound B	0.1 mg/L	[85]
		MIP-CDs	human blood	propranolol	-	[86]
		M-CDs@MIPs	bovine urine	bovine hemoglobin	17.3 nmol/L	[87]
		N-CDs@SiO <sub>2</sub> @MIPs	human urine and saliva	Asp	0.198 mg/L	[88]
	AIE-MIPs	urine	cathinone	0.3 $\mu$ mol/L	[89]	
	SPR	SPR-LDF-nanoMIP	human serum	HTR	4 fmol/L	[31]
		nanoMIP-Au	human blood	hemoglobin	$3.5 \times 10^{-4}$ mg/mL	[59]
		nanoMIP-Au	urine	copper(II) ion	-	[90]
	SERS	AuNCs@MIP	tablet	paracetamol	300 nmol/L	[14]
		AuNSs-MIP	biological fluid	trypsin enzyme	$4.1 \times 10^{-3}$ $\mu$ g/L	[60]
MIMC@Ag		dog saliva	cortisol	$10^{-7}$ mol/L	[91]	
CL	EuS NCs, K <sub>2</sub> S <sub>2</sub> O <sub>8</sub>	human serum	HIV-1 DNA	0.3 fmol/L	[55]	
	NiNCs-MIP@GO-Fe <sub>3</sub> O <sub>4</sub> , TPrA	human serum and urine	creatinine	0.5 nmol/L	[56]	
	CdS QDs, Luc	human urine	furosemide	4 nmol/L	[57]	
	TCPO-IMZ-H <sub>2</sub> O <sub>2</sub>	porcine urine	beta-agonists	0.3 pg/mL	[92]	
	MPA-Cu NCs	biological samples	enrofloxacin	27 pmol/L	[93]	
GO/TiO <sub>2</sub> -Ru(bpy) <sub>3</sub> <sup>2+</sup> @PEI-CdS	human serum, bird's nest	sialic acid	0.017 nmol/L	[94]		
Environmental safety	Fluorescent	MINs@PEGDA	environmental water	antibiotics	6.86 $\mu$ mol/L	[12]
		QD@SiO <sub>2</sub> @mSiO <sub>2</sub>	environmental water	malachite green	17.0 nmol/L	[19]
		MIP-QDs	electronic waste	TBBPA	3.6 ng/g	[61]
		MIP-CDs	river water	bisphenol A	30 nmol/L	[95]
		fluorescent MIP	environmental water	2,4-D	16.8 nmol/L	[96]
		MCOFs@MIPs@CDs	environmental water	2,4,6-trinitrophenol	100 pmol/L	[97]
	SiO <sub>2</sub> -APTES-FITC@MIPs	environmental water	lambda-cyhalothrin	10.26 nmol/L	[98]	
	SPR	Ag-PEI MIP	air	3-nitrotoluene	1.37 ng/mL	[99]
		MIP-Au film	seawater	Enterococcus faecalis	100 bacteria/mL	[100]
	SERS	SiO <sub>2</sub> @TiO <sub>2</sub> @Ag@MIPs	river water	pyrethroid	0.2 nmol/L	[21]
Ag@MOF/PDA-MIPs		river water	orange II	$10^{-10}$ mol/L	[62]	
Fe <sub>3</sub> O <sub>4</sub> @SiO <sub>2</sub> -Au@Ag		soil	paclobutrazol	0.075 $\mu$ g/g	[101]	
CL	MIP/CsPbBr <sub>3</sub> -QDs	aquaculture products	prometryn	5.0 pg/g	[48]	
	MWCNT/Cu/CDs	water	Co <sup>2+</sup>	$3.07 \times 10^{-10}$ mol/L	[63]	
	MIP-Fe <sub>3</sub> O <sub>4</sub> -NCs	seawater and fish	bisphenol A	$2.0 \times 10^{-4}$ $\mu$ g/L	[102]	

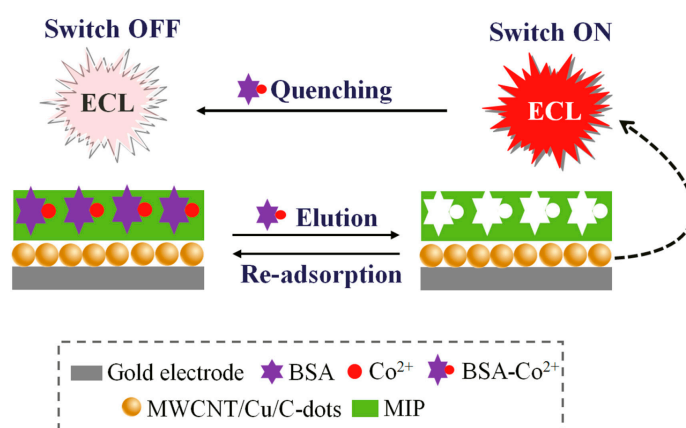


**Figure 9.** Dual-recognition switch sensor for the detection of Co<sup>2+</sup> [63]. Copyright 2019 Elsevier (Amsterdam, The Netherlands).

### 3. Conclusions

This article provides an up-to-date review of the construction process, detection principle, and application of four kinds of MIP optical sensors (fluorescence, SPR, SERS, and CL). Optical sensing methods have the advantage of being able to be portable and used in situ. MIP has the advantage of a high specificity and stability. The combination of the two can be used to detect a variety of substances with high speed, selectivity, sensitivity, and reproducibility. In recent years, there have been many innovations in the forms and applications of MIP optical sensors. From the aspect of optical materials, an increasing number of novel optical materials and functional monomers with excellent properties are applied, which further improves the sensitivity and stability of MIP optical sensors, and also expands their range of application. In terms of auxiliary components, the addition of optical fibers, smartphones, and other items greatly strengthens the flexibility of MIP optical sensors. MIP optical sensors can be applied outside of the laboratory, in real-world settings, including in even thousands of households. In terms of detection objects, in recent years, MIP optical sensors still mainly focus on food analysis, healthcare, and environmental safety. Objects with a wide range of properties, from ions to bacteria, can already be detected using MIP optical sensors.

However, MIP optical sensors still face many challenges. From the perspective of sensor construction, although most MIP optical sensors are easy to use and have good reproducibility, their preparation process remains complex and time-consuming, which limits their large-scale commercial production. Under the premise that the time of chemical synthesis is difficult to shorten, one way to solve this problem is to miniaturize the detection element as much as possible, so that the synthesis of the sensor, the detection of the target object, and the regeneration of the sensor can be carried out simultaneously and on a large scale. From the exploration of detection principle, most of the current articles explain the selectivity of MIP optical sensors from the aspects of steric hindrance and binding energy; thus, the interaction of MIPs with target molecules has been well explored. However, at present, few articles have studied in depth the effect of MIP on the properties of optical materials and the possible interactions between optical materials and target molecules. Although this may not affect our continued expansion of the application of MIP optical sensors, the clarification of these problems will certainly have profound guiding significance for the construction of sensors. From an application point of view, MIP optical sensors are very successful in identifying one substance or a class of similar substances. However, in practical application, we may need to face complex systems and many different analytes. Therefore, it is necessary to expand the multiple detection capability of MIP optical sensors. There are two possible ways to achieve this goal. One is to load multiple MIPs on the same MIP optical sensor and ensure that different target molecules can generate distinct optical signals when they contact the sensor. The other is to realize the integration of multiple

MIP optical sensors and pre-processing technology, so that the entire sensor system can accurately and continuously separate and detect various targets in the complex system. In addition, most of the current MIP optical sensors have good detection performance, but cannot work under extreme conditions. It is a difficult task to make MIP optical sensors capable of real-time monitoring under extreme conditions through proper design.

In summary, MIP optical sensors have been proven to be capable of efficient analysis. Next, we need to tap their potential and realize their mass production, and even mass application. We believe that with the efforts of many researchers around the world, this will be achieved in the near future.

**Author Contributions:** X.H.: Methodology, Data curation, Investigation, Writing—original draft preparation.; L.X.: Visualization, Funding acquisition, Writing—review and editing.; G.L.: Visualization, Resources, Funding acquisition, Supervision, Project administration, Writing—review and editing. All authors have read and agreed to the published version of the manuscript.

**Funding:** This research was funded by the State Key Program of National Natural Science foundation of China (No. 22134007), the National Natural Science Foundation of China (Nos. 21976213 and 22076223), the National Key Research and Development Program of China (No. 2019YFC1606101), and the Research and Development Plan for Key Areas of Food Safety in Guangdong Province of China (No. 2019B020211001).

**Institutional Review Board Statement:** Not applicable.

**Informed Consent Statement:** Not applicable.

**Data Availability Statement:** The data that support the findings of this study are available from the corresponding author upon reasonable request.

**Conflicts of Interest:** The authors declare no conflict of interest.

## References

1. Arshady, R.; Mosbach, K. Synthesis of substrate-selective polymers by host-guest polymerization. *Die Makromol. Chem.* **1981**, *182*, 687–692. [[CrossRef](#)]
2. Schirhagl, R. Bioapplications for Molecularly Imprinted Polymers. *Anal. Chem.* **2014**, *86*, 250–261. [[CrossRef](#)] [[PubMed](#)]
3. Chen, Y.; Xia, L.; Liang, R.; Lu, Z.; Li, L.; Huo, B.; Li, G.; Hu, Y. Advanced materials for sample preparation in recent decade. *TrAC Trends Anal. Chem.* **2019**, *120*, 115652. [[CrossRef](#)]
4. Turiel, E.; Martín-Esteban, A. Molecularly imprinted polymers-based microextraction techniques. *TrAC Trends Anal. Chem.* **2019**, *118*, 574–586. [[CrossRef](#)]
5. Wackerlig, J.; Lieberzeit, P.A. Molecularly imprinted polymer nanoparticles in chemical sensing—Synthesis, characterisation and application. *Sens. Actuators B Chem.* **2015**, *207*, 144–157. [[CrossRef](#)]
6. Ahmad, O.S.; Bedwell, T.S.; Esen, C.; Garcia-Cruz, A.; Piletsky, S.A. Molecularly Imprinted Polymers in Electrochemical and Optical Sensors. *Trends Biotechnol.* **2019**, *37*, 294–309. [[CrossRef](#)]
7. Rachkov, A.; McNiven, S.; El'skaya, A.; Yano, K.; Karube, I. Fluorescence detection of  $\beta$ -estradiol using a molecularly imprinted polymer. *Anal. Chim. Acta* **2000**, *405*, 23–29. [[CrossRef](#)]
8. Chen, C.; Wang, X.; Zhang, Y.; Li, X.; Gao, H.; Waterhouse, G.I.N.; Qiao, X.; Xu, Z. A molecularly-imprinted SERS sensor based on a TiO<sub>2</sub>@Ag substrate for the selective capture and sensitive detection of tryptamine in foods. *Food Chem.* **2022**, *394*, 133536. [[CrossRef](#)]
9. Chen, C.; Wang, X.; Waterhouse, G.I.N.; Qiao, X.; Xu, Z. A surface-imprinted surface-enhanced Raman scattering sensor for histamine detection based on dual semiconductors and Ag nanoparticles. *Food Chem.* **2022**, *369*, 130971. [[CrossRef](#)]
10. Akgönüllü, S.; Armutcu, C.; Denizli, A. Molecularly imprinted polymer film based plasmonic sensors for detection of ochratoxin A in dried Figure. *Polym. Bull.* **2022**, *79*, 4049–4067. [[CrossRef](#)]
11. Castro-Grijalba, A.; Montes-García, V.; Cordero-Ferradás, M.J.; Coronado, E.; Pérez-Juste, J.; Pastoriza-Santos, I. SERS-Based Molecularly Imprinted Plasmonic Sensor for Highly Sensitive PAH Detection. *ACS Sens.* **2020**, *5*, 693–702. [[CrossRef](#)]
12. Huang, Q.-D.; Lv, C.-H.; Yuan, X.-L.; He, M.; Lai, J.-P.; Sun, H. A novel fluorescent optical fiber sensor for highly selective detection of antibiotic ciprofloxacin based on replaceable molecularly imprinted nanoparticles composite hydrogel detector. *Sens. Actuators B Chem.* **2021**, *328*, 129000. [[CrossRef](#)]
13. Bakhshpour, M.; Göktürk, I.; Bereli, N.; Yılmaz, F.; Denizli, A. Selective Detection of Penicillin G Antibiotic in Milk by Molecularly Imprinted Polymer-Based Plasmonic SPR Sensor. *Biomimetics* **2021**, *6*, 72. [[CrossRef](#)]

14. Decorbie, N.; Tijunelyte, I.; Gam-Derouich, S.; Solard, J.; Lamouri, A.; Decorse, P.; Felidj, N.; Gauchotte-Lindsay, C.; Rinnert, E.; Mangeney, C.; et al. Sensing Polymer/Paracetamol Interaction with an Independent Component Analysis-Based SERS-MIP Nanosensor. *Plasmonics* **2020**, *15*, 1533–1539. [[CrossRef](#)]
15. Göktürk, I.; Bakhshpour, M.; Çimen, D.; Yılmaz, F.; Bereli, N.; Denizli, A. SPR Signal Enhancement with Silver Nanoparticle-Assisted Plasmonic Sensor for Selective Adenosine Detection. *IEEE Sens. J.* **2022**, *22*, 14862–14869. [[CrossRef](#)]
16. Pan, Y.; Liu, X.; Liu, J.; Wang, J.; Liu, J.; Gao, Y.; Ma, N. Chemiluminescence sensors based on molecularly imprinted polymers for the determination of organophosphorus in milk. *J. Dairy Sci.* **2022**, *105*, 3019–3031. [[CrossRef](#)]
17. He, H.; Muhammad, P.; Guo, Z.; Peng, Q.; Lu, H.; Liu, Z. Controllably prepared molecularly imprinted core-shell plasmonic nanostructure for plasmon-enhanced fluorescence assay. *Biosens. Bioelectron.* **2019**, *146*, 111733. [[CrossRef](#)]
18. Yang, Y.-Y.; Li, Y.-T.; Li, X.-J.; Zhang, L.; Kouadio Fodjo, E.; Han, S. Controllable in situ fabrication of portable AuNP/mussel-inspired polydopamine molecularly imprinted SERS substrate for selective enrichment and recognition of phthalate plasticizers. *Chem. Eng. J.* **2020**, *402*, 125179. [[CrossRef](#)]
19. Gui, W.; Wang, H.; Liu, Y.; Ma, Q. Ratiometric fluorescent sensor with molecularly imprinted mesoporous microspheres for malachite green detection. *Sens. Actuators B Chem.* **2018**, *266*, 685–691. [[CrossRef](#)]
20. Jia, B.J.; He, X.; Cui, P.L.; Liu, J.X.; Wang, J.P. Detection of chloramphenicol in meat with a chemiluminescence resonance energy transfer platform based on molecularly imprinted graphene. *Anal. Chim. Acta* **2019**, *1063*, 136–143. [[CrossRef](#)]
21. Li, H.; Wang, Y.; Li, Y.; Zhang, J.; Qiao, Y.; Wang, Q.; Che, G. Fabrication of pollutant-resistance SERS imprinted sensors based on SiO<sub>2</sub>@TiO<sub>2</sub>@Ag composites for selective detection of pyrethroids in water. *J. Phys. Chem. Solids* **2020**, *138*, 109254. [[CrossRef](#)]
22. Tian, H.; Li, Z.; Wang, C.; Xu, P.; Xu, S. Construction and Application of Molecularly Imprinted Fluorescence Sensor. *Prog. Chem.* **2022**, *34*, 593–608.
23. Shu, J.; Tang, D. Current Advances in Quantum-Dots-Based Photoelectrochemical Immunoassays. *Chem. Asian J.* **2017**, *12*, 2780–2789. [[CrossRef](#)] [[PubMed](#)]
24. Zhang, X.; Tang, B.; Li, Y.; Liu, C.; Jiao, P.; Wei, Y. Molecularly Imprinted Magnetic Fluorescent Nanocomposite-Based Sensor for Selective Detection of Lysozyme. *Nanomaterials* **2021**, *11*, 1575. [[CrossRef](#)] [[PubMed](#)]
25. Bahari, D.; Babamiri, B.; Salimi, A. Ultrasensitive molecularly imprinted fluorescence sensor for simultaneous determination of CA125 and CA15–3 in human serum and OVCAR-3 and MCF-7 cells lines using Cd and Ni nanoclusters as new emitters. *Anal. Bioanal. Chem.* **2021**, *413*, 4049–4061. [[CrossRef](#)]
26. Lu, H.; Xu, S. Ultrasensitive turn on molecularly imprinted fluorescence sensor for glycoprotein detection based on nanoparticles signal amplification. *Sens. Actuators B Chem.* **2020**, *306*, 127566. [[CrossRef](#)]
27. Liu, G.; Huang, X.; Li, L.; Xu, X.; Zhang, Y.; Lv, J.; Xu, D. Recent Advances and Perspectives of Molecularly Imprinted Polymer-Based Fluorescent Sensors in Food and Environment Analysis. *Nanomaterials* **2019**, *9*, 1030. [[CrossRef](#)]
28. Homola, J.; Yee, S.S.; Gauglitz, G. Surface plasmon resonance sensors: Review. *Sens. Actuators B Chem.* **1999**, *54*, 3–15. [[CrossRef](#)]
29. Wang, J.; Lin, W.; Cao, E.; Xu, X.; Liang, W.; Zhang, X. Surface Plasmon Resonance Sensors on Raman and Fluorescence Spectroscopy. *Sensors* **2017**, *17*, 2719. [[CrossRef](#)]
30. Akgönüllü, S.; Yavuz, H.; Denizli, A. Development of Gold Nanoparticles Decorated Molecularly Imprinted-Based Plasmonic Sensor for the Detection of Aflatoxin M1 in Milk Samples. *Chemosensors* **2021**, *9*, 363. [[CrossRef](#)]
31. Arcadio, F.; Seggio, M.; Del Prete, D.; Buonanno, G.; Mendes, J.; Coelho, L.C.C.; Jorge, P.A.S.; Zeni, L.; Bossi, A.M.; Cennamo, N. A Plasmonic Biosensor Based on Light-Diffusing Fibers Functionalized with Molecularly Imprinted Nanoparticles for Ultralow Sensing of Proteins. *Nanomaterials* **2022**, *12*, 1400. [[CrossRef](#)]
32. Nivedha, S.; Babu, P.R.; Senthilnathan, K. Surface plasmon resonance physics and technology. *Curr. Sci.* **2018**, *115*, 56–63. [[CrossRef](#)]
33. Wang, Z.; Zhang, W.; Liu, X.; Li, M.; Lang, X.; Singh, R.; Marques, C.; Zhang, B.; Kumar, S. Novel Optical Fiber-Based Structures for Plasmonics Sensors. *Biosensors* **2022**, *12*, 1016. [[CrossRef](#)]
34. Cennamo, N.; Maniglio, D.; Tatti, R.; Zeni, L.; Bossi, A.M. Deformable molecularly imprinted nanogels permit sensitivity-gain in plasmonic sensing. *Biosens. Bioelectron.* **2020**, *156*, 112126. [[CrossRef](#)]
35. Cennamo, N.; Arcadio, F.; Seggio, M.; Maniglio, D.; Zeni, L.; Bossi, A.M. Spoon-shaped polymer waveguides to excite multiple plasmonic phenomena: A multisensor based on antibody and molecularly imprinted nanoparticles to detect albumin concentrations over eight orders of magnitude. *Biosens. Bioelectron.* **2022**, *217*, 114707. [[CrossRef](#)]
36. Arcadio, F.; Zeni, L.; Minardo, A.; Eramo, C.; Di Ronza, S.; Perri, C.; D’Agostino, G.; Chiaretti, G.; Porto, G.; Cennamo, N. A Nanoplasmonic-Based Biosensing Approach for Wide-Range and Highly Sensitive Detection of Chemicals. *Nanomaterials* **2021**, *11*, 1961. [[CrossRef](#)]
37. Zhang, J.; Li, S. Molecularly imprinted polymers-surface-enhanced Raman spectroscopy: State of the art and prospects. *Int. J. Environ. Anal. Chem.* **2022**, *102*, 1385–1415. [[CrossRef](#)]
38. Raman, C.V.; Krishnan, K.S. A New Type of Secondary Radiation. *Nature* **1928**, *121*, 501–502. [[CrossRef](#)]
39. Fleischmann, M.; Hendra, P.J.; McQuillan, A.J. Raman spectra of pyridine adsorbed at a silver electrode. *Chem. Phys. Lett.* **1974**, *26*, 163–166. [[CrossRef](#)]
40. Zhang, L.; Guo, Y.; Hao, R.; Shi, Y.; You, H.; Nan, H.; Dai, Y.; Liu, D.; Lei, D.; Fang, J. Ultra-rapid and highly efficient enrichment of organic pollutants via magnetic mesoporous nanosponge for ultrasensitive nanosensors. *Nat. Commun.* **2021**, *12*, 6849. [[CrossRef](#)]

41. Guo, X.; Li, J.; Arabi, M.; Wang, X.; Wang, Y.; Chen, L. Molecular-Imprinting-Based Surface-Enhanced Raman Scattering Sensors. *ACS Sens.* **2020**, *5*, 601–619. [[CrossRef](#)] [[PubMed](#)]
42. Kantarovich, K.; Tsarfati, I.; Gheber, L.A.; Haupt, K.; Bar, I. Writing Droplets of Molecularly Imprinted Polymers by Nano Fountain Pen and Detecting Their Molecular Interactions by Surface-Enhanced Raman Scattering. *Anal. Chem.* **2009**, *81*, 5686–5690. [[CrossRef](#)] [[PubMed](#)]
43. Feng, S.; Gao, F.; Chen, Z.; Grant, E.; Kitts, D.D.; Wang, S.; Lu, X. Determination of  $\alpha$ -Tocopherol in Vegetable Oils Using a Molecularly Imprinted Polymers–Surface-Enhanced Raman Spectroscopic Biosensor. *J. Agric. Food Chem.* **2013**, *61*, 10467–10475. [[CrossRef](#)] [[PubMed](#)]
44. Wang, Z.; Yan, R.; Liao, S.; Miao, Y.; Zhang, B.; Wang, F.; Yang, H. In situ reduced silver nanoparticles embedded molecularly imprinted reusable sensor for selective and sensitive SERS detection of Bisphenol A. *Appl. Surf. Sci.* **2018**, *457*, 323–331. [[CrossRef](#)]
45. Sun, M.; Su, Y.; Lv, Y. Advances in chemiluminescence and electrogenerated chemiluminescence based on silicon nanomaterials. *Luminescence* **2020**, *35*, 978–988. [[CrossRef](#)]
46. Chen, J.; Qiu, H.; Zhao, S. Fabrication of chemiluminescence resonance energy transfer platform based on nanomaterial and its application in optical sensing, biological imaging and photodynamic therapy. *TrAC Trends Anal. Chem.* **2020**, *122*, 115747. [[CrossRef](#)]
47. He, T.; Wang, G.N.; Liu, J.X.; Zhao, W.L.; Huang, J.J.; Xu, M.X.; Wang, J.P.; Liu, J. Dummy molecularly imprinted polymer based microplate chemiluminescence sensor for one-step detection of Sudan dyes in egg. *Food Chem.* **2019**, *288*, 347–353. [[CrossRef](#)]
48. Zhang, R.-R.; Gan, X.-T.; Xu, J.-J.; Pan, Q.-F.; Liu, H.; Sun, A.-L.; Shi, X.-Z.; Zhang, Z.-M. Ultrasensitive electrochemiluminescence sensor based on perovskite quantum dots coated with molecularly imprinted polymer for prometryn determination. *Food Chem.* **2022**, *370*, 131353. [[CrossRef](#)]
49. Zou, L.; Ding, R.; Li, X.; Miao, H.; Xu, J.; Pan, G. Typical Fluorescent Sensors Exploiting Molecularly Imprinted Hydrogels for Environmentally and Medicinally Important Analytes Detection. *Gels* **2021**, *7*, 67. [[CrossRef](#)]
50. Akgönüllü, S.; Yavuz, H.; Denizli, A. SPR nanosensor based on molecularly imprinted polymer film with gold nanoparticles for sensitive detection of aflatoxin B1. *Talanta* **2020**, *219*, 121219. [[CrossRef](#)]
51. Erdem, Ö.; Cihangir, N.; Saylan, Y.; Denizli, A. Comparison of molecularly imprinted plasmonic nanosensor performances for bacteriophage detection. *New J. Chem.* **2020**, *44*, 17654–17663. [[CrossRef](#)]
52. Perçin, I.; Idil, N.; Bakhshpour, M.; Yilmaz, E.; Mattiasson, B.; Denizli, A. Microcontact Imprinted Plasmonic Nanosensors: Powerful Tools in the Detection of Salmonella paratyphi. *Sensors* **2017**, *17*, 1375. [[CrossRef](#)]
53. Wang, J.; Li, J.; Zeng, C.; Qu, Q.; Wang, M.; Qi, W.; Su, R.; He, Z. Sandwich-Like Sensor for the Highly Specific and Reproducible Detection of Rhodamine 6G on a Surface-Enhanced Raman Scattering Platform. *ACS Appl. Mater. Interfaces* **2020**, *12*, 4699–4706. [[CrossRef](#)]
54. Cai, Y.; He, X.; Cui, P.L.; Liu, J.; Li, Z.B.; Jia, B.J.; Zhang, T.; Wang, J.P.; Yuan, W.Z. Preparation of a chemiluminescence sensor for multi-detection of benzimidazoles in meat based on molecularly imprinted polymer. *Food Chem.* **2019**, *280*, 103–109. [[CrossRef](#)]
55. Babamiri, B.; Salimi, A.; Hallaj, R. A molecularly imprinted electrochemiluminescence sensor for ultrasensitive HIV-1 gene detection using EuS nanocrystals as luminophore. *Biosens. Bioelectron.* **2018**, *117*, 332–339. [[CrossRef](#)]
56. Babamiri, B.; Salimi, A.; Hallaj, R.; Hasanzadeh, M. Nickel nanoclusters as a novel emitter for molecularly imprinted electrochemiluminescence based sensor toward nanomolar detection of creatinine. *Biosens. Bioelectron.* **2018**, *107*, 272–279. [[CrossRef](#)]
57. Zhang, Y.; Cui, Y.; Sun, M.; Wang, T.; Liu, T.; Dai, X.; Zou, P.; Zhao, Y.; Wang, X.; Wang, Y.; et al. Deep learning-assisted smartphone-based molecularly imprinted electrochemiluminescence detection sensing platform: Portable device and visual monitoring furosemide. *Biosens. Bioelectron.* **2022**, *209*, 114262. [[CrossRef](#)]
58. Li, W.; Zhang, H.; Chen, S.; Liu, Y.; Zhuang, J.; Lei, B. Synthesis of molecularly imprinted carbon dot grafted YVO<sub>4</sub>:Eu<sup>3+</sup> for the ratiometric fluorescent determination of paranitrophenol. *Biosens. Bioelectron.* **2016**, *86*, 706–713. [[CrossRef](#)]
59. Saylan, Y.; Denizli, A. Molecular Fingerprints of Hemoglobin on a Nanofilm Chip. *Sensors* **2018**, *18*, 3016. [[CrossRef](#)]
60. Arabi, M.; Ostovan, A.; Zhang, Z.; Wang, Y.; Mei, R.; Fu, L.; Wang, X.; Ma, J.; Chen, L. Label-free SERS detection of Raman-Inactive protein biomarkers by Raman reporter indicator: Toward ultrasensitivity and universality. *Biosens. Bioelectron.* **2021**, *174*, 112825. [[CrossRef](#)]
61. Feng, J.; Tao, Y.; Shen, X.; Jin, H.; Zhou, T.; Zhou, Y.; Hu, L.; Luo, D.; Mei, S.; Lee, Y.-I. Highly sensitive and selective fluorescent sensor for tetrabromobisphenol-A in electronic waste samples using molecularly imprinted polymer coated quantum dots. *Microchem. J.* **2019**, *144*, 93–101. [[CrossRef](#)]
62. Xue, Y.; Shao, J.; Sui, G.; Ma, Y.; Li, H. Rapid detection of orange II dyes in water with SERS imprinted sensor based on PDA-modified MOFs@Ag. *J. Environ. Chem. Eng.* **2021**, *9*, 106317. [[CrossRef](#)]
63. Li, S.; Li, J.; Ma, X.; Pang, C.; Yin, G.; Luo, J. Molecularly imprinted electroluminescence switch sensor with a dual recognition effect for determination of ultra-trace levels of cobalt (II). *Biosens. Bioelectron.* **2019**, *139*, 111321. [[CrossRef](#)]
64. Hou, J.; Li, H.; Wang, L.; Zhang, P.; Zhou, T.; Ding, H.; Ding, L. Rapid microwave-assisted synthesis of molecularly imprinted polymers on carbon quantum dots for fluorescent sensing of tetracycline in milk. *Talanta* **2016**, *146*, 34–40. [[CrossRef](#)] [[PubMed](#)]
65. Zhao, C.; Ren, Y.; Li, G. Detection of naringin by fluorescent polarization molecularly imprinted polymer. *Polym. Bull.* **2022**, *80*, 1411–1424. [[CrossRef](#)]

66. Wang, Y.; Wang, J.; Cheng, R.; Sun, L.; Dai, X.; Yan, Y. Synthesis of molecularly imprinted dye-silica nanocomposites with high selectivity and sensitivity: Fluorescent imprinted sensor for rapid and efficient detection of  $\tau$ -fluvastatin in vodka. *J. Sep. Sci.* **2018**, *41*, 1880–1887. [[CrossRef](#)]
67. Li, M.; Shen, F.; Zhang, Z.; Ren, X. A Novel 2-Acrylamide-6-Methoxybenzothiazole Fabricated Molecularly Imprinted Polymers for Direct Fluorescent Sensing of Alachlor. *Chromatographia* **2016**, *79*, 71–78. [[CrossRef](#)]
68. Lu, H.; Xu, S. Visualizing BPA by molecularly imprinted ratiometric fluorescence sensor based on dual emission nanoparticles. *Biosens. Bioelectron.* **2017**, *92*, 147–153. [[CrossRef](#)]
69. Zeni, L.; Pesavento, M.; Marchetti, S.; Cennamo, N. [INVITED] Slab plasmonic platforms combined with Plastic Optical Fibers and Molecularly Imprinted Polymers for chemical sensing. *Opt. Laser Technol.* **2018**, *107*, 484–490. [[CrossRef](#)]
70. Neng, J.; Xu, K.; Wang, Y.; Jia, K.; Zhang, Q.; Sun, P. Sensitive and Selective Detection of New Red Colorant Based on Surface-Enhanced Raman Spectroscopy Using Molecularly Imprinted Hydrogels. *Appl. Sci.* **2019**, *9*, 2672. [[CrossRef](#)]
71. Mugo, S.M.; Lu, W. Determination of  $\beta$ -Estradiol by Surface-Enhanced Raman Spectroscopy (SERS) Using a Surface Imprinted Methacrylate Polymer on Nanoporous Biogenic Silica. *Anal. Lett.* **2022**, *55*, 378–387. [[CrossRef](#)]
72. Yin, W.; Wu, L.; Ding, F.; Li, Q.; Wang, P.; Li, J.; Lu, Z.; Han, H. Surface-imprinted  $\text{SiO}_2$ @Ag nanoparticles for the selective detection of BPA using surface enhanced Raman scattering. *Sens. Actuators B Chem.* **2018**, *258*, 566–573. [[CrossRef](#)]
73. Hua, M.Z.; Feng, S.; Wang, S.; Lu, X. Rapid detection and quantification of 2,4-dichlorophenoxyacetic acid in milk using molecularly imprinted polymers–surface-enhanced Raman spectroscopy. *Food Chem.* **2018**, *258*, 254–259. [[CrossRef](#)]
74. Xu, Y.; Hassan, M.M.; Ali, S.; Li, H.; Chen, Q. SERS-based rapid detection of 2,4-dichlorophenoxyacetic acid in food matrices using molecularly imprinted magnetic polymers. *Microchim. Acta* **2020**, *187*, 454. [[CrossRef](#)]
75. Jiang, Z.Q.; Cai Zhang, H.; Zhang, X.Y.; Ping Wang, J. Determination of Tetracyclines in Milk with a Molecularly Imprinted Polymer-Based Microtiter Chemiluminescence Sensor. *Anal. Lett.* **2019**, *52*, 1315–1327. [[CrossRef](#)]
76. Xu, J.; Zhang, R.; Liu, C.; Sun, A.; Chen, J.; Zhang, Z.; Shi, X. Highly Selective Electrochemiluminescence Sensor Based on Molecularly Imprinted-quantum Dots for the Sensitive Detection of Cyfluthrin. *Sensors* **2020**, *20*, 884. [[CrossRef](#)]
77. Li, Z.B.; Liu, J.; Liu, J.X.; Wang, Z.H.; Wang, J.P. Determination of sulfonamides in meat with dummy-template molecularly imprinted polymer-based chemiluminescence sensor. *Anal. Bioanal. Chem.* **2019**, *411*, 3179–3189. [[CrossRef](#)]
78. Huang, J.J.; Liu, J.; Liu, J.X.; Wang, J.P. A microtitre chemiluminescence sensor for detection of pyrethroids based on dual-dummy-template molecularly imprinted polymer and computational simulation. *Luminescence* **2020**, *35*, 120–128. [[CrossRef](#)]
79. Jia, B.-J.; Huang, J.; Liu, J.-X.; Wang, J.-P. Detection of chloramphenicol in chicken, pork and fish with a molecularly imprinted polymer-based microtiter chemiluminescence method. *Food Addit. Contam. Part A* **2019**, *36*, 74–83. [[CrossRef](#)]
80. Wang, S.; Zhao, P.; Li, N.; Qiao, X.; Xu, Z. Development of a chemiluminescence sensor based on molecular imprinting technology for the determination of trace monocrotophos in vegetables. *Adv. Polym. Technol.* **2018**, *37*, 1401–1409. [[CrossRef](#)]
81. Zhang, T.; Liu, J.; Wang, J.P. Preparation of a molecularly imprinted polymer based chemiluminescence sensor for the determination of amantadine and rimantadine in meat. *Anal. Methods* **2018**, *10*, 5025–5031. [[CrossRef](#)]
82. Wang, Q.; Li, S.; Li, J. A molecularly imprinted sensor with enzymatic enhancement of electrochemiluminescence of quantum dots for ultratrace clopyralid determination. *Anal. Bioanal. Chem.* **2018**, *410*, 5165–5172. [[CrossRef](#)] [[PubMed](#)]
83. Zhao, Y.; Chen, Y.; Fang, M.; Tian, Y.; Bai, G.; Zhuo, K. Silanized carbon dot-based thermo-sensitive molecularly imprinted fluorescent sensor for bovine hemoglobin detection. *Anal. Bioanal. Chem.* **2020**, *412*, 5811–5817. [[CrossRef](#)] [[PubMed](#)]
84. Zhang, X.; Yang, S.; Jiang, R.; Sun, L.; Pang, S.; Luo, A. Fluorescent molecularly imprinted membranes as biosensor for the detection of target protein. *Sens. Actuators B Chem.* **2018**, *254*, 1078–1086. [[CrossRef](#)]
85. Ma, Y.; Wang, H.; Guo, M. Preparation of ECB Molecularly Imprinted Film Fluorescent Sensor for Detection of Traditional Chinese Herbal Medicine. *Chem. J. Chin. Univ.* **2019**, *40*, 1381.
86. Hariati, R.; Rezaei, B.; Jamei, H.R.; Ensafi, A.A. Manufacturing of a Sensitive and Selective Optical Sensor Based on Molecularly Imprinted Polymers and Green Carbon Dots Synthesized from Cedrus Plant for Trace Analysis of Propranolol. *Anal. Sci.* **2019**, *35*, 1083–1088. [[CrossRef](#)]
87. Lv, P.; Xie, D.; Zhang, Z. Magnetic carbon dots based molecularly imprinted polymers for fluorescent detection of bovine hemoglobin. *Talanta* **2018**, *188*, 145–151. [[CrossRef](#)]
88. Peng, L.; Xu, Y.; Huang, T.; Liu, X.; Yang, X.; Meng, M.; Yan, Y. Molecularly Imprinted Fluorescent Sensors Based on Nitrogen-Doped CDs for Highly Selective Detection of Aspirin. *Nano* **2020**, *16*, 2150019. [[CrossRef](#)]
89. Hu, R.; Yan, Y.; Jiang, L.; Huang, C.; Shen, X. Determination of total cathinones with a single molecularly imprinted fluorescent sensor assisted by electromembrane microextraction. *Microchim. Acta* **2022**, *189*, 324. [[CrossRef](#)]
90. Safran, V.; Göktürk, I.; Derazshamshir, A.; Yilmaz, F.; Sağlam, N.; Denizli, A. Rapid sensing of  $\text{Cu}^{2+}$  in water and biological samples by sensitive molecularly imprinted based plasmonic biosensor. *Microchem. J.* **2019**, *148*, 141–150. [[CrossRef](#)]
91. Fan, L.; Wang, Z.; Zhang, Y.; Song, Y.; Yang, H.; Wang, F. Molecularly imprinted Monolithic column-based SERS sensor for selective detection of cortisol in dog saliva. *Talanta* **2022**, *249*, 123609. [[CrossRef](#)] [[PubMed](#)]
92. Xu, M.X.; Li Zhao, W.; Liu, J.; He, T.; Huang, J.J.; Ping Wang, J. Determination of  $\beta$ -Agonists in Porcine Urine by Molecularly Imprinted Polymer Based Chemiluminescence. *Anal. Lett.* **2019**, *52*, 1771–1787. [[CrossRef](#)]
93. Wang, D.; Jiang, S.; Liang, Y.; Wang, X.; Zhuang, X.; Tian, C.; Luan, F.; Chen, L. Selective detection of enrofloxacin in biological and environmental samples using a molecularly imprinted electrochemiluminescence sensor based on functionalized copper nanoclusters. *Talanta* **2022**, *236*, 122835. [[CrossRef](#)] [[PubMed](#)]

94. Cao, N.; Zhao, F.; Zeng, B. A novel ratiometric molecularly imprinted electrochemiluminescence sensor for sensitive and selective detection of sialic acid based on PEI-CdS quantum dots as anodic coreactant and cathodic luminophore. *Sens. Actuators B Chem.* **2020**, *313*, 128042. [[CrossRef](#)]
95. Liu, G.; Chen, Z.; Jiang, X.; Feng, D.-Q.; Zhao, J.; Fan, D.; Wang, W. In-situ hydrothermal synthesis of molecularly imprinted polymers coated carbon dots for fluorescent detection of bisphenol A. *Sens. Actuators B Chem.* **2016**, *228*, 302–307. [[CrossRef](#)]
96. Limaee, N.Y.; Rouhani, S.; Olya, M.E.; Najafi, F. Selective Recognition of Herbicides in Water Using a Fluorescent Molecularly Imprinted Polymer Sensor. *J. Fluoresc.* **2020**, *30*, 375–387. [[CrossRef](#)]
97. Wang, M.; Gao, M.; Deng, L.; Kang, X.; Zhang, K.; Fu, Q.; Xia, Z.; Gao, D. A sensitive and selective fluorescent sensor for 2,4,6-trinitrophenol detection based on the composite material of magnetic covalent organic frameworks, molecularly imprinted polymers and carbon dots. *Microchem. J.* **2020**, *154*, 104590. [[CrossRef](#)]
98. Wang, J.; Qiu, H.; Shen, H.; Pan, J.; Dai, X.; Yan, Y.; Pan, G.; Sellergren, B. Molecularly imprinted fluorescent hollow nanoparticles as sensors for rapid and efficient detection  $\lambda$ -cyhalothrin in environmental water. *Biosens. Bioelectron.* **2016**, *85*, 387–394. [[CrossRef](#)]
99. Aznar-Gadea, E.; Rodríguez-Canto, P.J.; Martínez-Pastor, J.P.; Lopatynskiy, A.; Chegel, V.; Abargues, R. Molecularly Imprinted Silver Nanocomposites for Explosive Taggant Sensing. *ACS Appl. Polym. Mater.* **2021**, *3*, 2960–2970. [[CrossRef](#)]
100. Erdem, Ö.; Saylan, Y.; Cihangir, N.; Denizli, A. Molecularly imprinted nanoparticles based plasmonic sensors for real-time *Enterococcus faecalis* detection. *Biosens. Bioelectron.* **2019**, *126*, 608–614. [[CrossRef](#)]
101. Kou, Y.; Wu, T.; Zheng, H.; Kadasala, N.R.; Yang, S.; Guo, C.; Chen, L.; Liu, Y.; Yang, J. Recyclable Magnetic MIP-Based SERS Sensors for Selective, Sensitive, and Reliable Detection of Paclitaxel Residues in Complex Environments. *ACS Sustain. Chem. Eng.* **2020**, *8*, 14549–14556. [[CrossRef](#)]
102. Zhang, R.-R.; Zhan, J.; Xu, J.-J.; Chai, J.-Y.; Zhang, Z.-M.; Sun, A.-L.; Chen, J.; Shi, X.-Z. Application of a novel electrochemiluminescence sensor based on magnetic glassy carbon electrode modified with molecularly imprinted polymers for sensitive monitoring of bisphenol A in seawater and fish samples. *Sens. Actuators B Chem.* **2020**, *317*, 128237. [[CrossRef](#)]

**Disclaimer/Publisher's Note:** The statements, opinions and data contained in all publications are solely those of the individual author(s) and contributor(s) and not of MDPI and/or the editor(s). MDPI and/or the editor(s) disclaim responsibility for any injury to people or property resulting from any ideas, methods, instructions or products referred to in the content.